

Detection of polarized mm and sub-mm emission from Sgr A*D.K. Aitken^{1,4}, J. Greaves², Antonio Chrysostomou^{1,2}W. Holland¹, J.H. Hough², D. Pierce-Price³J. Richer³**ABSTRACT**

We report the detection of linear polarization from Sgr A* at 750, 850, 1350 and 2000 μ m which confirms the contribution of synchrotron radiation. From the lack of polarization at longer wavelengths it appears to arise in the millimetre/sub-millimetre excess. There are large position angle changes between the millimetre and sub-millimetre results and these are discussed in terms of a polarized dust contribution in the sub-millimetre and various synchrotron models. In the model which best explains the data the synchrotron radiation from the excess is self-absorbed in the millimetre region and becomes optically thin in the sub-millimetre. This implies that the excess arises in an extremely compact source ~ 2 Schwarzschild radii.

Subject headings: Galaxy: centre–Synchrotron radiation–Sgr A*

1. Introduction

Observations of stellar proper motions in the vicinity of Sgr A* (Ghez et al. 1998), the non-thermal radio source at the apparent centre of the Galaxy, show that its mass of $\sim 2.5 \times 10^6 M_{\odot}$ is highly compact on a scale < 0.01 pc, reinforcing its claim to be a massive black-hole candidate. The spectrum of Sgr A* extends as a rough power law $\sim \nu^{\alpha}$, where α lies between $\frac{1}{4}$ and $\frac{1}{3}$, from a low-frequency turn-over at a few GHz up to ~ 100 GHz, (e.g. Mezger, Duschl and Zylka 1996 and references therein), and above this frequency there is evidence of a mm to sub-mm excess over this power law extending almost to the atmospheric cut-off near 1000 GHz (Serabyn et al. 1997, Falcke et al. 1998). The nature of the mm/sub-mm excess has been discussed by Serabyn et al. (1997)

¹Dept. of Physical Sciences, University of Hertfordshire, Hatfield, Herts, AL10 9AB, U.K.

²Joint Astronomy Centre, 660 N. A‘ohokū Place, University Park, Hilo, HI 96720, U.S.A.

³Cavendish Laboratory, Madingley Road, Cambridge, CB3 0HE, U.K.

⁴email: d.aitken@star.herts.ac.uk

and the possibility that it is due to dust is effectively eliminated: at 1.3mm its size is less than 1 arcsecond with an implied brightness temperature in excess of 100 K, inconsistent with the shorter wavelength data, and the implication is that there are two separate synchrotron components.

The radio spectrum of Sgr A* has for some years been modelled in various ways in terms of synchrotron radiation but searches for linear polarization, the characteristic signature of this mechanism, have only recently been reported. Bower et al. (1999a,b) used the VLA at 4.8, 8.4, 22 and 43 GHz in its spectropolarimetric mode and the BIMA array at 86 GHz finding upper limits of <0.2% at the lower frequencies and <1% at 86 GHz. These small upper limits on linear polarization, given the sensitivity of the observations to large rotation measures due to Faraday rotation ($RM \sim 10^7$ rad m^{-2} at 8.4 GHz), are difficult to account for and this is discussed at length by Bower et al. (1999a). Apart from this there has been only a marginal detection at 800 μm of $4.9 \pm 3.2\%$ at $129 \pm 19^\circ$ (Flett and Murray 1991) and a report of circular polarization at 4.8 GHz by Bower et al. (1999c).

In mm to sub-mm polarimetric imaging studies of the central 15 pc of the Galaxy we have detected linear polarization in Sgr A* at 750, 850, 1350 and 2000 μm which we present here. Discussion of the field distribution in the circum-nuclear disk (CND) and neighbouring molecular clouds as revealed by these observations will be presented separately.

2. Observations and Results

The observations were made using the SCUBA camera (Holland et al. 1999) and its polarimeter (Greaves et al. 1999) on the 15m James Clerk Maxwell Telescope (JCMT) in Hawaii. SCUBA observes simultaneously with arrays of 37 and 91 bolometers, at either 850 and 450 μm respectively, or 750 and 350 μm with a change of filters. Polarimetric observations were made in imaging mode at all four submillimetre wavelengths, and single-point polarimetry towards Sgr A* was also done at 1.35 and 2mm, using single bolometers and supplementing the data with small grid maps. The arrays have fields of view of 2.3 arcmin, and full-width half-maximum beam sizes range from 7–8'' at the shortest wavelengths to 34'' at 2 mm (Table 1).

Observations were made by chopping the secondary mirror at 7.8 Hz to remove the mean sky level, and nodding between left and right beams at slower rates to take out sky gradients. For polarimetry, a rotating half-wave plate and fixed etched grid were used to modulate the signal seen by the detectors. Polarimetry at 750 and 850 μm resulted in a Nyquist-sampled image after 32s of integration, after which the waveplate was stepped by 22.5° . The single-pixel data were observed in a similar manner but with 8s of integration per waveplate angle. Total integration times were 5–10 complete waveplate cycles, or 15–85 minutes. The data were reduced using the SURF (Jenness and Lightfoot 1998) and POLPACK (Starlink user note 223) software packages; for each pixel a sinusoidal modulation is fitted to deduce the source percentage and direction (p, θ) of the polarization.

From observations of Saturn and Uranus, during the run and from archival data, the instrumental polarization is found to be close to 1% and known to ± 0.1 – 0.2 % at a given wavelength and elevation. At 450 and $1350\mu\text{m}$ the instrumental polarizations are larger (3.5 and 2.7% respectively due to wind blind structure) but still known to 0.2 to 0.8% respectively. The planets were assumed to be unpolarized and a limited check was made on this for Saturn where sky rotation can be used to separate instrumental from any planetary polarization. While we cannot exclude the possibility that Saturn is slightly polarized this introduces an error of less than 0.3% in the instrumental polarization subtraction. The instrumental polarization changes by only 0.1% over the elevation range used and the uncertainties in the corrected polarization is considered good to $\pm 0.1 - 0.2\%$. Errors in the absolute orientation of the waveplate are one degree or less.

Intensity calibration at 1350 and $2000\mu\text{m}$ was obtained using Uranus taking the brightness temperatures as 96K and 110K respectively, and at $850\mu\text{m}$ from Mars taking $T_B = 208\text{K}$. Since the emphasis is on the polarimetric results, we did not perform extremely accurate calibration observations, but typical uncertainties are only about ± 10 %. For the $750\mu\text{m}$ data Saturn was used for calibration taking $T_B=123\text{K}$ and a greater error was introduced since this planet is larger than the beam; we note that the $750\mu\text{m}$ flux for Sgr A* appears anomalously low. Atmospheric transmission was measured with skydips.

A fundamental limitation is the maximum chop throw of $180''$ (in this case at a position angle of 145° east of north), which proved to be insufficient at 350 and $450\mu\text{m}$. Surrounding dust emission has a steep spectral index (Pierce-Price et al., 2000) resulting in increasing off-beam contamination at these shortest wavelengths where Sgr A* was not detected above background. At $850\mu\text{m}$ the off-beam signals are only 15% of the Sgr A* flux and these uncertainties should be similar or smaller at 750, 1350 and $2000\mu\text{m}$ at all of which Sgr A* was clearly detected. During the observation period the field of view rotates but the chop orientation on the sky is maintained; thus every spatial point in the map retains the same chop positions in α and δ although different array bolometers may be involved. The results of polarimetric imaging in the vicinity of Sgr A* are presented in Table 1 and the total flux at the position of Sgr A* is given in column 3.

There will in general be two contributions to the background, namely from cool dust in the inner cavity and the edges of the CND and free-free emission from the HII region Sgr A West, predominantly from the central ionized filaments.

Dust and free-free emission contribute significantly to the observed flux but in this wavelength region there is no independent evidence at sufficient resolution to determine the contribution of the dust emission component in the central beams. In the sub-mm the flux in annuli from one to two beam radii were determined from the images and at 1350 and $2000\mu\text{m}$ observations in eight beams circumferentially distributed about SgrA* sampled the ambient flux between 1.7–3.7 beam radii from SgrA*. Estimates of the free-free contribution in the central beams and these peripheral areas were made from the 2 arcsecond resolution 3.6cm radio continuum maps of Roberts and Goss (1993), after removing the Sgr A* point source itself. These fluxes were then

scaled to the present wavelengths as $\nu^{-0.1}$, appropriate for optically thin free-free emission, and the approximation is made that the central dust contribution is just that derived from the peripheral regions after subtraction of the free-free component (column 7 in the table). The flux from SgrA* after subtraction of the dust and free-free contributions (column 8) will also include any local dust excess (or deficit) over background. Since at 2mm the correction for free-free is large due to the large beam size the reliability of the non-thermal flux estimate at this wavelength will be affected.

The observed E vector polarizations and position angles (north through east) are listed in Table 1 in columns 9 and 10. At $450\mu\text{m}$ there is general polarization over the central 30 arcseconds with no significant change at the position of Sgr A* and its average $\sim 3\%$ at a position angle of 100° (E vector) is attributed to dust. At wavelengths between 750 and $2000\mu\text{m}$ the polarization at the position of Sgr A* is well detected at the $10\text{-}\sigma$ level. In the sub-mm it stands out from its surroundings and is clearly associated with the flux peak at the position of Sgr A*. This can be seen in Fig 1 which shows the central $80 \times 100''$ region about Sgr A* at $850\mu\text{m}$. At 1350 and $2000\mu\text{m}$ the observations are from single pointed observations where the HII region Sgr A West and Sgr A* are the dominant sources in the beam and Sgr A* is the only significant contributor to polarization.

3. Interpretation

At $2000\mu\text{m}$, and to a lesser extent at $1350\mu\text{m}$, there are only two contributors to the flux: diffuse free-free emission and Sgr A* itself. Since the former is unpolarized the polarization observed confirms the synchrotron nature of Sgr A*; it also suggests that the polarization is only associated with the mm/sub-mm excess since it has not been observed at wavelengths of 3.5mm and longer where the power-law spectrum dominates. Note that at $2000\mu\text{m}$ the largest contributor is from free-free emission and therefore the intrinsic polarization of SgrA* must be large.

A large difference of position angle between the mm and sub-mm observations is evident in Table 1 and various ways of understanding this are next investigated.

Although the mm position angles themselves are very close the three shortest wavelength position angles define a straight line when plotted against λ^2 ; if a rotation of π is subtracted from the 2mm angle a rough linear relation is maintained. However the rotation measure then indicated is so large ($-1.44 \times 10^6 \text{ rad/m}^2 = \pi/(\lambda_2^2 - \lambda_{1.35}^2)$) that polarization within the band pass of 40GHz at 2mm would be undetectable. Therefore the closeness of the mm position angles indeed indicate that there is little if any Faraday rotation.

Changes in polarization and position angle with time are well documented in the compact cores of blazars and some AGN (e.g. Saikia and Salter 1988) and also have been observed at mm wavelengths (Nartallo et al. 1998). Sgr A* is known to be variable on a time scale of months. While there is a separation of some months between the observations presented here, those at 750 , 1350 and $2000\mu\text{m}$ were all made in August 1999 within a week and these do show the large position

angle difference between the mm and sub-mm polarizations. Furthermore, the $850\mu\text{m}$ observation in March also lies on the same trend of position angle with wavelength. Variability is therefore unlikely to have been a significant influence on the position angle, although it seems possible that Sgr A* may have increased in brightness during this period.

Since the sub-mm dust emission is polarized it will affect the observed polarization and it is tempting to try to attribute the whole position angle change to dust.

Denoting by I_o , I_d and I_s the observed central flux, the estimated dust and Sgr A* components respectively and by q_o , q_d and q_s their Stokes q parameters, the synchrotron component q_s can be found from

$$I_o q_o = I_d q_d + I_s q_s$$

and similarly for the Stokes u components.

It is difficult to estimate the dust contribution to polarization from the 750 and $850\mu\text{m}$ observations because of the proximity of Sgr A* and its high intrinsic polarization. Instead we use the $450\mu\text{m}$ observations in which Sgr A* is not detected, and the polarization is $\sim 3\%$ at a position angle of $\sim 100^\circ$. There are some problems here with polarized flux in the reference beams but other indicators of dust alignment in the central parsec are consistent with this estimate: observations at $350\mu\text{m}$ (Novak et al. 2000) yield 1.9% at 87° near the position of SgrA*, and at $100\mu\text{m}$ the results are similar (Hildebrand et al. 1993) though both these are in a larger beam; the only information at high resolution is from the mid-infrared (Aitken et al. 1996) where integrations over a central 14 arcsecond diameter yield 2.4% at 125° , admittedly weighted to warm dust.

The intrinsic polarization resulting from removing the unpolarized free-free contribution and adopting 3% at 100° for dust emission is shown in Table 1 columns 11 and 12. At mm wavelengths these numbers are insensitive to the uncertainties in the adopted dust polarization and even in the submm the range of dust polarizations given in the previous paragraph changes the intrinsic polarization by $\pm 3\%$ at most and less than $\pm 3^\circ$. Similarly uncertainties in the relative fractions of the three flux components has little effect on the intrinsic position angle but changing dilution does introduce errors to the intrinsic polarization fraction and at 750 and $2000\mu\text{m}$ the upper bounds are poorly defined. In Table 1 the errors to the intrinsic polarization are derived by assuming $\pm 15\%$ errors to the free-free and $\pm 20\%$ errors to the dust contributions except at $2000\mu\text{m}$ where the adopted error is $\pm 40\%$ (these dust contribution errors are derived from the observed variation in the peripheral flux). It is clear that dust polarization cannot explain the abrupt change of position angle between the mm and sub-mm, rather it is increased and it approaches $\pi/2$.

We can turn the above argument around to determine what dust polarization is needed in the sub-mm to cause the position angle shift given the intrinsic synchrotron polarization of the mm results, say $\sim 10\%$ at 85° . With the $850\mu\text{m}$ fluxes and polarization given in Table 1 the required dust polarization is then 12.0% at 163° , larger than any dust emission polarization yet observed. It might be argued that this could be due to unusual conditions close to Sgr A* and an additional dust component in the central beam. Any such emission is already included in the Table 1 entry

for Sgr A* and because the same polarized intensity ($\sim 450\text{mJy}$) has to be supplied from much less dust emission the required polarization would be in excess of 25%.

An assumption made so far is that throughout the wavelength region of these observations the synchrotron radiation remains either optically thin or self-absorbed. Most models of the synchrotron SED in Sgr A* consider the mm/sub-mm excess to be self absorbed but it may well be that at the shortest wavelengths it becomes optically thin. In that case the synchrotron position angle shifts through 90° and becomes close to 175° in the sub-mm. The dust corrected sub-mm points are now discrepant by 6 to 14° and this could be attributed to the crudeness of the correction.

Approximating the synchrotron emitting region by a simple slab with constant energy density and magnetic field we find (e.g. Ginzburg and Syrovatskii 1965, 1969, Pacholczyk and Swihart 1967) that for the polarization to change sign near 1mm then ν_{ssa} , the synchrotron self absorption frequency, lies in the range 0.6–0.7mm, close to the peak of the mm/sub-mm excess, and the required fields, densities and energies are similar to those in the compact source models of Beckert and Duschl (1997). The polarization transition of this simple model is quite sharp, as is observed, with the polarization quickly approaching saturation on the long wavelength side, changing sign near 1mm and steadily rising at shorter wavelengths.

A variant on this explanation is that self-absorption results in different optical depths with possibly different field distributions being probed as a function of wavelength. In that case, however, one should encounter diminishing polarization towards shorter wavelengths due to the superposition of a range of field orientations, and this is not observed.

4. Discussion

Synchrotron radiation from Sgr A* has been detected between $750\mu\text{m}$ and $2000\mu\text{m}$ with an intrinsic polarization $\sim 10\%$. This polarization arises from the spectral region of the mm/sub-mm excess. The present observations are compounded by the presence of polarized emission from dust and dilution by free-free emission in these large beams. Although this has led to a number of possible explanations for the large position angle shift between the mm and sub-mm results all but one of these can be eliminated: the closeness of the position angles at 1.35 and 2mm require that there is little or no Faraday rotation, dust polarization can only produce a small shift which is in the wrong sense, and the shift is not due to variability. Only a transition between optically thin synchrotron radiation in the sub-mm and self-absorption in the mm region appears as a plausible explanation of the shift. Future small beam observations will be needed to confirm this result.

A puzzle re-emphasized here is the lack of polarization at 3.5mm (Bower et al. 1999a,b) and longer wavelengths in view of the large intrinsic polarization of Sgr A* at 1.35 and 2mm. Sufficient dilution of the mm/sub-mm excess to bring it below 1% requires not only a steeply falling spectrum with decreasing frequency for the excess, where $\nu^{5/2}$ is expected for self absorption, but also that the cut-off frequency of the power-law section is below 2mm to ensure a fast rising flux of the

power law region. It is possible, as well, that a flare in Sgr A* at 100GHz in March 1998 (Tsuboi, Miyazaki and Tsutsumi 1998) has affected the result of Bower et al. 1999b.

The synchrotron self-absorption transition in the sub-mm proposed here is consistent with the model of the excess by Beckert and Duschl (1997), and requires the excess to arise from a compact source ~ 2 Schwarzschild radii in size. Also because of the transition the $\pi/2$ ambiguity of the relationship between position angle and magnetic field is removed and hence the field orientation is close to east-west, since at mm wavelengths the emission is considered self-absorbed.

5. Conclusions

We report the observation of millimetre and sub-millimetre polarization from Sgr A*, confirming the role of synchrotron radiation. The polarization is a property of the mm/sub-mm excess, demonstrating that the excess is real and not an artefact of variability and that it and the power-law spectrum arise in distinct structures. There is a large position angle shift between the mm and sub-mm observations. This can be explained by a transition between optically thin and self absorbed synchrotron radiation near 1 mm. Such a high self-absorption frequency implies a very compact source $\sim 2R_S$.

We are grateful to the UK Panel for Allocation of Telescope Time for the award of observing time for this project. JSR acknowledges a Royal Society Fellowship and DP-P a PPARC Research Studentship. The JCMT is operated by the Joint Astronomy Centre on behalf of PPARC of the UK, the Netherlands OSR, and NRC Canada. The authors would like to thank the NCSA Astronomy Digital Image Library (ADIL) for providing images for this paper. We thank an unknown referee for useful comments.

REFERENCES

- Aitken, D.K., Smith, C.H., Moore, T.J.T., Roche, P.F., 1996, in “The Galactic Center”, ed R. Gredel, ASP Conf Ser 102, 179
- Aitken, D.K., Gezari, D.Y., Smith, C.H., McCaughrean, M.J., Roche, P.F., 1991, ApJ, 380, 419
- Beckert, T., Duschl, W.J., 1997, A&A, 328, 95
- Beckert, T., Duschl, W.J., Mezger, P.G., Zylka, R., 1996, A&A, 307, 450
- Bower, G.C., Backer, D.C., Zhao, J-H., Goss, M., Falcke, H., 1999a, ApJ, 521, 582)
- Bower, G.C., Wright, C.H., Backer, D.C., Falcke, H., 1999b, ApJ, (in press)
- Bower, G.C., Falcke, H., Backer, D.C., 1999c, ApJ, 523, L29

- Falcke, H., Goss, W.M., Matsuo, H., Teuben, P., Zhao, J-H., Zylka, R., *ApJ*, 1998, 499, 731
- Flett, Murray, 1991, *MNRAS*, 249, 4P
- Ghez, A., Klein, B.L., Morris, M., Becklin, E.E., 1998, *ApJ*, 509, 678
- Ginzburg, V.L., Syrovatskii, S.I., 1965, *ARA&A*, 3, 297
- Ginzburg, V.L., Syrovatskii, S.I., 1969, *ARA&A*, 7, 375
- Greaves, J.S., Jenness, T., Chrysostomou, A., Holland, W.S., Berry, D.S., 1999, in “Imaging at Radio through Submillimeter Wavelengths”, ed J. Magnum et al., *ASP Conf Ser* (in press)
- Hildebrand, R.H., in “Interstellar Dust”, *IAU Symp 135*, eds L.J.Allamandola, Tielens,A.G.G.M., Kluwer, Dordrecht, p275
- Hildebrand, R.H., Davidson, J.A., Dotson, J., Figer, D.F., Novak, G., Platt, S.R., Tao, L., 1993, *ApJ*, 417, 565
- Holland, W.S., Robson, E.I., Gear, W.K., Cunningham, C.R., Lightfoot, J.F., Jenness, T., Ivison, R.J., Stevens, J.A., Ade, P.A.R., Griffin, M.J., Duncan, W.D., Murphy, J.A., Naylor, D.A., 1999, *MNRAS*, 303, 659
- Jenness, T., Lightfoot, J.F., 1998, in *ASP Conf Ser 145, Astronomical Data Analysis Software and Systems*, ed R.Albrecht, R.N. Hook, H.A. Bushouse (San Francisco: ASP), 216
- Krichbaum, T.P., Graham, D.A., Witzel, A., Greve, A., Wink, J.E., Grewing, M., Colomer, F., de Vicente, P., Gomez-Gonzalez, J., Baudry, A., Zensus, J.A., 1998, *A&A*, 335, L106
- Melia, F., 1994, *ApJ*, 426, 577
- Mezger, P.G., Duschl, W.J., Zylka, R., 1996, *A&A Rev*, 7, 289
- Narayan, R., Mahadevan, R., Grindlay, J.E., Popham, R.G., and Gammie, C., 1998, *ApJ*, 492, 554
- Nartallo, R., Gear, W.K., Murray, A.G., Robson, E.I., Hough, J.H., 1998, *MNRAS*, 297, 667
- Novak, G., Dotson, J.L., Dowell, C.D., Hildebrand, R.H., Renbarger, T., Schkeunung, D.A., 2000, *ApJ*, 529, 241
- Pacholczyk, A.G., Swihart, T.L., 1967, *ApJ*, 150, 647
- Pierce-Price et al., 2000 (in preparation)
- Rees, M.J., 1982, in “The Galactic Center”, ed G.R.Riegler & R.D.Blandford(New York:AIP) 166
- Roberts, D.A., Goss, W.M., 1993, *ApJS*, 86, 133
- Saikia, D.J., Salter, C.J., 1988, *ARA&A*, 26, 93

Sault, H.J., Macquart, J.P., preprint

Serabyn, E., Carlstrom, J., Lay, O., Lis, D.C., Hunter, T.R., Lacy, J.H., Hills, R.E., 1997, *ApJ*, 490, L77

Tsuboi, Miyasaki, Tsutsumi, 1998, in “Galactic Center Workshop” ASP Conf Series, in press

Zylka, R., Mezger, P.G., 1988, *A&A*, 190, L25

Galactic Centre

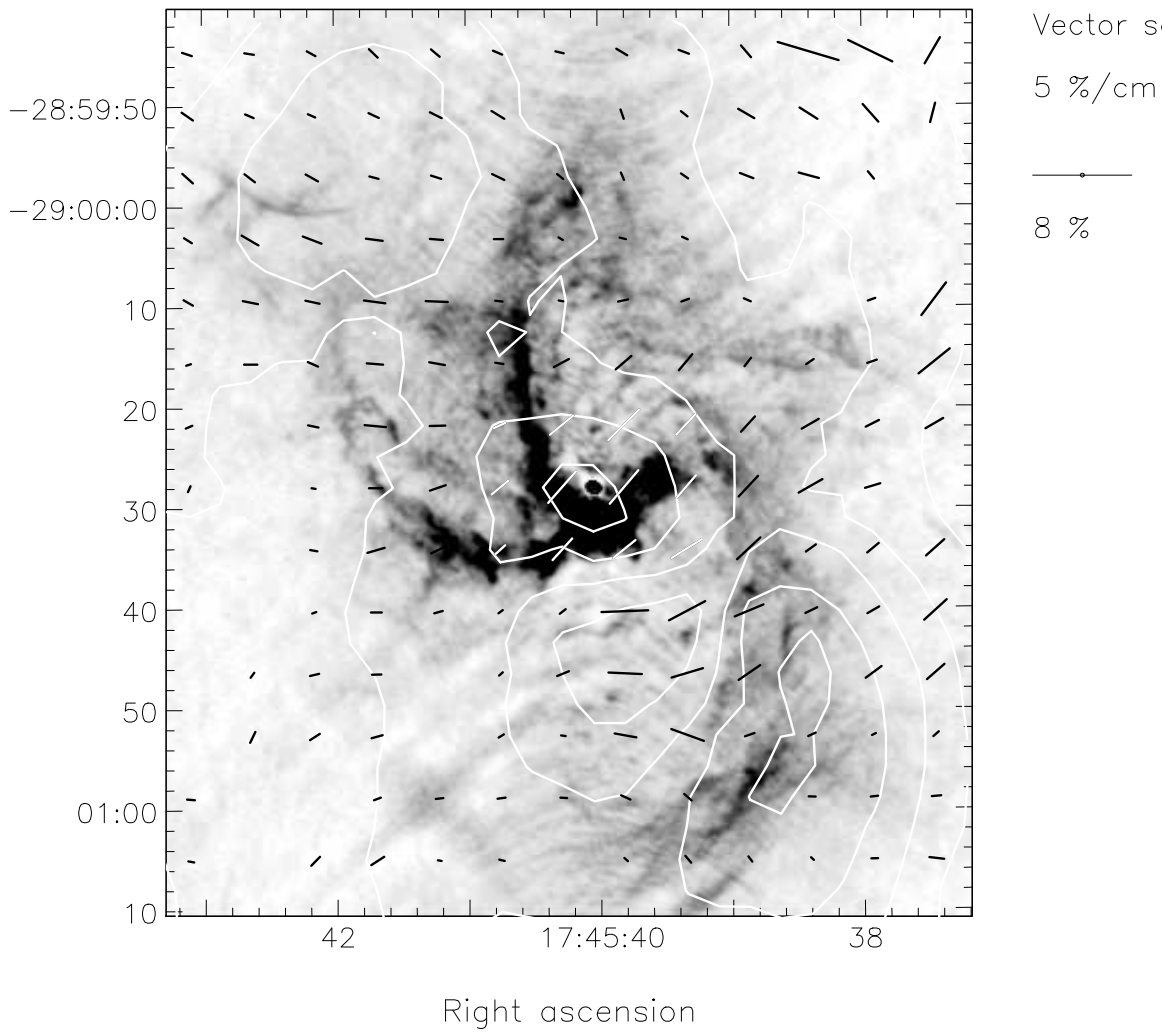


Fig. 1.— Greyscale image of 3.6 cm emission (Roberts & Goss 1993, courtesy of ADIL) overlaid with contours of the 850 μm emission from the central region around Sgr A * , which is clearly seen as a point source in the centre of this image. The short lines on the figure show the magnitude and direction of the sub-millimetre polarisation \mathbf{E} -vector. Note how the magnitude of the polarisation is larger at the position of Sgr A * (more than one large vector is seen as the beam is bigger than the vector spacing in this figure). Coordinates for SgrA * are $17^{\text{h}} 45^{\text{m}} 40.049^{\text{s}}$, $-29^{\circ} 00' 27.98''$ (J2000).

Table 1. **Sgr A* fluxes**

λ μm	beam arcsec	central flux (Jy/beam)			ambient free-free	central dust	Sgr A* 8 =3-4-6 =4+6-5	obs. polarsn.		intr. polarsn.		date
		total	excess	free-free				P(%)	$\theta(^{\circ})$	P(%)	$\theta(^{\circ})$	
1	2	3	4 ^a	5	6	7 ^b	8	9	10	11	12	13
750	12.5 ^c	~5	~2.5	2.5	1	~1.5	$\sim 1 \pm 0.5$	3.8 ± 0.4	164 ± 3	22^{+25}_{-9}	169 ± 3	27 Aug 99
850	14	8.2	3.6	2.25	0.95	3.65	2.3 ± 0.9	3.3 ± 0.2	150 ± 2	13^{+10}_{-4}	161 ± 3	25 Mar 99
1350	22.5	6.5	4.9	3.55	0.85	0.75	2.2 ± 0.5	4.1 ± 0.4	89 ± 3	11^{+3}_{-2}	88 ± 3	22 Aug 99
2000	33.5	8.0	6.4	5.8	1.2	0.4	1.8 ± 0.9	2.9 ± 0.3	84 ± 3	12^{+9}_{-4}	83 ± 3	22 Aug 99

^a(central excess)=(central total)-(ambient)

^bflux from the central dust component is taken as equal to the flux from the ambient dust

^cfluxes were measured in a 16 arcsec beam

Note. — Errors on observed P and θ are 1σ statistical errors. See text for uncertainty estimates on Sgr A* flux and intrinsic polarisations.